Validation of Dripline Emitter Characteristics and Pump Performance Curve for Network Analysis

Validation of Dripline Emitter Characteristics and Pump Performance Curve for Network Analysis

Yeboah Gyasi-Agyei

Central Queensland University, School of Engineering and Technology, Rockhampton, QLD 4702, Australia. E-mail: y.gyasi-agyei@cqu.edu.au

Abstract

In this paper, simple methods for validating the emitter characteristics of driplines and pump performance curves for dripline network design and simulation are presented. Pressure compensating driplines were tested and used to aid grass establishment to control erosion on the steep slopes of a newly constructed flood levee. The dripline networks consisted of several bays that had different lengths and numbers of lateral rows as dictated by fence lines of property boundaries and access road ramps. Single emitters as well as thousands in dripline networks were tested. It was observed that the average emitter discharge could exceed the supplier's value (2.1 l/h) by as much as 10%. Moreover, the emitter discharge value tended to be higher between the opening threshold pressure head of the pressure compensating emitters of 4 m and 10 m compared with those for pressure heads above 10 m. The emitter insertion head loss coefficient exhibited considerable variability (0.117 – 0.753) although the average value of 0.336 was close to the supplier's value of 0.36. The supplier's pump performance curve overestimated pressure head by 11 m for a flowrate of 50 l/min, but the overestimation decreased to 6 m at the higher flowrate of 300 l/min. Comparison of observed and

simulated pressures at strategic locations within the dripline networks were used to identify the emitter characteristics without the need for flow measurements. Simulation results were used to determine excessive bay inlet pressures and the corresponding ball valve opening fractions to drop the inlet pressure to an acceptable limit for each bay.

Introduction

Roma, the head office of the Maranoa Regional Council (MRC) in Queensland, Australia, with a population of 6,906 (2011 census) has a long history of significant flooding. Of particular interest are the 3 consecutive years of flooding in 2010, 2011, and 2012. Through funding from the Australian and Queensland Governments and from the MRC, a Stage 1 flood mitigation project consisting of 5.2 km of earthen levee (average height of 2.8 m) was constructed in 2014. Included in the design specification was topsoiling of the levee batters (steep slopes) and establishment of grasses to provide long-term stability of the batters against erosion, and also to provide an aesthetically pleasing environment. HEFRAIL (Mitigation of Hydrology and Erosion problems, and Fire Risks, within Central Queensland Railway Systems) processes were tailored to suit the conditions of the Roma levee batters in order to achieve the desired grass coverage of 90% or above. The HEFRAIL processes include surface preparation, soil treatment, seeding, and hydraulics modelling of water flow through driplines (Gyasi-Agyei et al., 2001; Gyasi-Agyei, 2003; Gyasi-Agyei, 2004a,b; Gyasi-Agyei, 2011). As a result of water scarcity in the arid environment, precision irrigation involving the use of drip laterals has been an integral part of HEFRAIL although sprinkler irrigation could be used in this instance. However, there were key elements of the Roma levee project that called for proper

46 investigations regarding various aspects of HEFRAIL. While the treatments imposed on the levee
47 batters for erosion control involved soil and water treatments, and seed mix design, only the dripline
48 network aspects are presented in this paper.
49
50 ***Dripline Network Set Up***
51 Roma, located at latitude 26°34′24″S and longitude 148°47′12″E, and at an elevation of 299.4
52 m above mean sea level, is 479 km from Brisbane, Queensland, Australia. Fig. 1 shows the Roma
53 township and the location of the levee. Five levee sections, indicated as Sites B, C, D, E and F in Fig.
54 1, were selected for treatment on both sides. However only Sites B and F were evaluated in this
55 paper. Four 5,000 l poly tanks were placed next to the levee at each site and filled with water from
56 the town water supply network during off peak periods. Fig. 2 shows the parallel arrangement of the
57 4 poly tanks at Site F. An irrigation control valve was installed to allow filling of the tanks at the
58 desired periods of the day as mentioned above. A float valve was installed inside the first tank to shut
59 off water supply inflow when the tanks were full. Although the town water supply is clean of
60 sediments that could harm the emitters of the driplines, filters were provided for security reasons.
61 The flood levee runs through several property boundaries with many fence lines and access
62 road ramps for crossing from one side to the other. These fence lines and ramps dictated the bay and
63 lateral lengths as it was difficult to lay the driplines across these geometric controls. HEFRAIL
64 processes recommend laying the driplines at intervals increasing from 0.5 m at the top to 2 m at the
65 bottom of the embankment batters. Because of a quick establishment of over 90% grass cover was
66 required, it was decided to use a constant interval of 1 m between the laterals. End sleeves were used
67 to seal the lateral ends by crimping the distal 0.2 m which also facilitated flushing of the laterals from
68 time to time. Where possible, pairs of bays were linked to the same water take off from the mains

in order to reduce the number of crossings at the top of the levee. Each bay has its own ball valve so that it can be isolated for maintenance as occasional blow outs due to loose joints and weak damaged sections that cannot be totally eliminated. Also, the ball valve can be used to regulate the inlet pressure of each bay, thus adjusting the pressures to within acceptable limits. Other specifications are the 25 mm secondary sub-mains from which the laterals take off and the 40 mm sub-mains that link the mains and the secondary lateral sub-mains. Hence the size of the mains was the only variable to be selected based on hydraulic simulation subject to the geometrical constraints, with the aim of minimising the time required for irrigation.

Fig. 3 depicts the design layout for the sites to be simulated to determine the desired mainline size to allow the minimum number of irrigation sessions. Poly pipe diameter sizes to choose from were 63 and 75 mm. Initial simulation indicated that frictional losses in the 50 mm or less diameter lines were too high, requiring shorter bay lengths and, thus, more bays to cover the batters; these sizes were therefore eliminated. Also, 90 mm and greater diameter poly pipes and their fittings are not readily available on the market and have delivery delays. Therefore, it was decided to use 63 mm mains for Site F which has the lowest levee height and 75 mm mains for Site B. Each irrigation site along the levee consisted of several bays of different lengths dictated by geometrical controls of property boundary fence lines and access roads as mentioned earlier. Hence the pressure distribution within the networks varied considerably and needed to be determined through simulation to aid in the operations of the irrigation networks.

Objectives

The emitter properties of a new dripline on the market that has a reported very low emitter insertion head loss coefficient were verified through laboratory tests of a few individual emitters,

while two lateral lengths and selected bays consisting of thousands of emitters were examined in the field. In addition, the pump performance curve was verified in the field. The objectives of the study were to:

- validate the emitter discharge parameter using a few single emitters, laterals lengths containing between 300 and 700 emitters (bays F6, F8), and combinations of bays containing between 3000 and 6500 emitters (bays F7, F9, F10);
- validate the emitter insertion head loss coefficient using lateral lengths containing between 300 and 700 emitters (bays F6, F8);
- validate the pump performance curve which is in turn used to estimate emitter discharge (Sites B and F, bays F7, F9, F10, B3, B11, B13, B14);
- simulate flows through dripline networks to ascertain pressure distribution to aid the design and operation of combinations of bays at the same time;
- provide a simple approach to estimate ball valve opening fraction of each bay to reduce the pressures to within acceptable limits during the operation of the dripline networks.

Materials and Methods

The Dripline Properties

Commercially available heavy duty non-draining pressure compensating anti-siphon dripline was sourced. It has the following properties:

- internal diameter of 19 mm;
- pressure compensating range of 5.1 m to 40.1 m;

- emitter spacing of 300 mm;
- nominal emitter discharge of 2.1 l/h;
- emitter insertion head loss coefficient of 0.36;
- standard coil length of 350 m.

There were variations in the levee heights as constructed and on the design plans used to construct the irrigation networks. Hence there was a shortfall in the 2.1 l/h driplines so 2.4 l/h dripline was use on sites D and E. These drip lateral specifications were chosen based on the experience with a previous railway corridor erosion control project. The lateral rolls were from the same manufacturing batch and, therefore, expected to have the same emitter type and hydraulic characteristics. This type of drip lateral is moulded from low-density polyethylene for flexibility and durability, and the emitters are enclosed and welded to the inside wall of the tubing as it is extruded in the manufacturing process. Its non-drain feature reduces time at start-up, making it suitable for short pulse irrigation cycles. The risk of soil being "vacuumed" into the dripper is reduced by its anti-siphon feature. Also, the risk of blockages is reduced by the emitter's "self-flushing" action at the beginning and end of each irrigation cycle.

Simple methods were used to establish the veracity of the manufacturers' published values of the emitter discharge and insertion head loss coefficient for all emitters. Thirteen pieces of lateral containing only one emitter each were cut from different rolls of the lateral for testing. The set up at a CQUniversity laboratory shown in Fig. 4 consisted of a cross pipe connecting a 140 mm diameter Bourdon pressure gauge, a sink water source, a piece of the lateral and an outflow pipe to the sink. Different pressures regulated by the two taps were applied to the emitter and the amount of water collected in a beaker over 15 minutes was weighed to estimate its volume, and hence the emitter discharge.

Pressure gauges were installed at the beginning and distal end of the 95 m and 209 m laterals at the top of bays F6 and F8, respectively, as shown in Fig. 3 to monitor pressure changes to be used to infer the emitter insertion head loss coefficient with the knowledge of elevation differences and the dripline blank tubing friction loss factor. The 63 mm diameter Bourdon pressure gauges used for the lateral pressure measurements have 0.2 m resolution (±1.6% accuracy). This resolution is small enough not to have any significant impact on the objectives of the study. A domestic water meter was used to monitor the total volume of water for 16 minutes in the 95 m and 209 m long laterals (effective length of 208 and 93.3 m, the rest occupied by the meter) at the top of F6 and F8, respectively, to infer the average emitter discharge. Different pressures were applied to the inlet of the lateral and the gauge values were recorded and used to establish the emitter insertion head loss coefficient.

The water meter was installed in the mains just after the ball valve controlling flow to the irrigation network (Fig. 2) at Site F to establish the pump rating curve. Identical pumps were used at all sites, so it was decided to test only one pump. Flow volumes over 15 minutes were recorded for several pressures at the pump, varying the flowrate, and hence the pump pressure, using the ball valve controlling flow to the drip network. Installation of the water meter restricted flow so flowrates above 165 l/min could not be measured. Note that all bay valves were opened to allow free flow of water from the pump. To extend the pump rating curve to flows up to 350 l/min, an ultrasonic flowmeter (±2% accuracy) that has a minimal head loss was used. It was installed at the same location as the water meter at Site F. This ultrasonic flowmeter displays instantaneous flowrate in l/s but exhibited some variability. No data logger was available, so sequences of photographs were taken of the displays over 2 minutes for each pump setting. A minimum of 30 display photographs per pump setting were viewed and the flowrates averaged to obtain representative values. With this equipment the required

pump performance rating curve range was observed. The interest was on the pressure input into the dripline network (pressure output from the pump), and this pressure reading was used. The poly tanks were 2 m high and only a couple of metres of poly pipe connected the tanks to the entry of the pump, hence the pump suction head losses were minimal, and compensated for by the water head in the tanks. Also, this flowmeter was used to monitor the flowrate in the 95 m lateral at F6 to infer the average emitter discharge and insertion head loss coefficient.

The Hydraulic Model for Simulation

There are several approaches in the literature on the hydraulic modelling of drip irrigation laterals (Wu and Gitlin, 1975; Warrick and Yitayew, 1988; Yitayew and Warrick, 1988; Hathoot et al., 1993, 2000; Kang and Nishiyama, 1996; Vallesquino and Luque-Escamilla, 2002; Carrión et al., 2013; Fernández García et al., 2015; Baiamonte, 2016). Baiamonte (2018) has provided a recent review on the hydraulics and design of drip irrigation laterals. However, the step-by-step approach (e.g., Hathoot et al., 1993) in which the hydraulic model is applied to segments working from one end to the other, and taking into account all head losses including the emitter head loss coefficient, was pursued. Computational demand was the initial drawback of the step-by-step method but, with the advancement in computing power, it was not an issue.

Inclusion of the emitter head loss coefficient has generated a lot of interest with different approaches emerging on how to estimate it. For example, Provenzano et al. (2007) used computational fluid dynamics to estimate it, while Juana et al. (2002) related it to the pipe and emitter dimensions. Demir et al. (2007) developed two mathematical models based on Buckingham's π theorem for

184 predicting local losses in drip laterals. Artificial neural networks have been used to develop
185 predictive models for local losses taking into account the geometrical characteristics of the pipe and
186 emitter (Marti et al., 2010). Gyasi-Agyei (2013) presented a Bayesian approach for estimating the
187 local head loss of laterals due to the emitter insertion. The range of the emitter insertion head loss
188 coefficient identified by the Bayesian approach (0.95 - 1.17) and that provided by the manufacturer
189 (0.95 - 1.12) were nearly identical. A complete dripline network is simulated here to optimise the
190 schedule of irrigation by running a combination of bays at the same time with due regard to the
191 dripline emitter operating pressure range.
192
193 ***Single Lateral***
194 The basic unit of the hydraulic modelling is the drip lateral which is simplified in Fig. 5 with
195 the inlet cut midway between two emitters. The emitter discharge is:

196 $$q_i = k H_i^x \quad (1)$$

197 where q_i is the emitter discharge (l/h), H_i is the pressure head (m) at emitter i, k is the emitter discharge
198 coefficient and x is the emitter discharge exponent characterising the flow regime and emitter type,
199 and has a value close to zero within the pressure compensating region. The backward step-by-step
200 application of the basic pipe friction head loss equation is used. Considering a lateral segment
201 separated by downstream node i and upstream node $i-1$, the energy equation is given as:

202 $$H_{i-1} = H_i + \left(\frac{8 s_i}{\pi^2 g d^5} f_i + \frac{\alpha}{2 g A^2} \right) Q_i^2 + s_i S_o \quad (2)$$

203 where Q_i is the discharge ($m^3 s^{-1}$), S_o is the constant slope of the lateral (positive for uphill and negative
204 for downhill), s_i (m) is the spacing between the nodes, A (m^2) is the cross-sectional area of the lateral,
205 d (m) is the lateral internal diameter, g (ms^{-2}) is the acceleration due to gravity, and f_i is the friction

coefficient for the segment. Local head loss due to emitter insertion is accounted for by the velocity head term ($\alpha V^2/2g=\alpha Q^2/(2g\ A^2)$) in Eq. (2), with α referred to as the emitter insertion head loss coefficient.

The friction coefficient *f*, is obtained by solving the Colebrook-White equation considered to be the most acceptable standard (Winning and Cools, 2013) for turbulent flow ($Re_i > 4000$) given as:

$$\frac{1}{\sqrt{f_i}} = -2\log\left(\frac{k_s}{3.7d}+\frac{2.51}{\mathrm{Re}_i\sqrt{f_i}}\right) \quad (3)$$

which is a function of the Reynolds number (Re), diameter (d), and roughness (k_s) which has a value of zero for smooth pipes. For laminar flow ($Re_i \leq 2000$) $f_i=64/Re_i$, and for the unstable zone ($2000 < Re \leq 4000$) it is obtained by linear interpolation between the lower limit of the laminar and the upper limit of the turbulent zones. For an assumed value of H_n (see Fig. 5), Eq. (1) is used to estimate the emitter discharge q_n which is set equal to Q_n. Because we are dealing with pressure compensating laterals, *x* in Eq. (1) was set to zero. Re_n is estimated and f_n is calculated with Eq. (3). Next, Eq. (2) is used to estimate H_{n-1}, then q_{n-1} with Eq. (1), and from the continuity principle $Q_{n-1} = Q_n - q_{n-1}$. The calculation is repeated for the next segment upstream until the entry of the lateral. Given an inlet pressure H_0, the last emitter head (H_n) is optimised to match H_0. If the optimised H_n value falls below the minimum value of the pressure compensating range, then H_0 is not appropriate. Note that the backward step-by-step method with optimization used here is found to be more efficient than the forward step-by-step method with root finding approach adopted in Gyasi-Agyei (2007; 2013).

Drip Network

For easy following of the explanation of the mathematical derivations on the hydraulic simulation of the dripline network, a hypothetical Site A consisting of 6 bays shown in Fig. 6 is

demonstrated. Each bay's inlet pressure and discharge depend on the inlet pressure of the last lateral of the bay. The secondary sub-main segments and laterals of the bay are numbered from upstream to downstream as shown in Fig. 6 for bay A1. Given the inlet pressure for the last lateral H_{S_n}, Q_{S_n} is estimated and this is the same flow through the segment S_{n-1}, noting that n=12 is the number of the secondary sub-main segments and laterals of bay A1. For the remaining secondary sub-main segments of the bay, $Q_{S_{i-2}} = Q_{S_{i-1}} + Q_{S_i}$ in accordance with the continuity principle where i is the bay segment number. The upstream pressure of the secondary sub-main segments is determined using the backward step-by-step equation given as:

$$H_{S_i} = H_{S_{i+1}} + \frac{k_{eS_{i+1}}}{2gA_{S_{i+1}}^2} Q_{S_{i+1}}^2 + f_{S_i} \frac{8L_{S_i}}{\pi^2 g d_{S_i}^5} Q_{S_i}^2 + L_{S_i} s_{S_i} \qquad (4)$$

where subscript S_i refers to bay segment i, f_{Si} and L_{Si} are the friction factor and length of bay segment S_i, and k_e is the total entry fitting (minor) head loss coefficient. k_e values were added depending on the number of fittings required at the entry connection; i.e., for 90° elbow (1.1), flow in line tee (0.35), all k_e values obtained from Vinidex design manual (http://www.vinidex.com.au/). Repeating the process gives the bay entry pressure and discharge of H_{S_1} and Q_{S_1} which are dependent on the value of H_{S_n}. The primary sub-main segments are first numbered, and the numbering continues with the mains segments as shown with numbers red in Fig. 6. Note that the primary sub-main segments 2 and 4 are dummies with length of zero to ensure not more than 3 segments meet at a junction. This is necessary because the mathematics follow a branching tree structure with one inflow and a maximum of two outflows at a junction. Also, there is no direct link between the mains and the bays, the sub-mains serving as bridges. Eq. (4) is then used to determine the pressures in the segments using subscript M_i for the sub-main and main segments to distinguish them from the values of the

bay inlet segments (A_iS_1), and the flows are added at junctions to satisfy the continuity principle. Equating pressures at junction inlets leads to finding the roots of a system of N equations where N is the number of bays. In the case of Fig. 6 which has 6 bays, the system of equations are given as:

$$
\begin{aligned}
H_{M_1} + \frac{ke_{M_1}}{2gA_{M_1}^{\ 2}} Q_{M_1}^2 \;-\; H_{M_2} - \frac{ke_{M_2}}{2gA_{M_2}^{\ 2}} Q_{M_2}^2 &= 0 \\
H_{A3S_1} + \frac{ke_{A3S_1}}{2gA_{A3S_1}^{\ 2}} Q_{A3S_1}^2 \;-\; H_{A4S_1} - \frac{ke_{A4S_1}}{2gA_{A4S_1}^{\ 2}} Q_{A4S_1}^2 &= 0 \\
H_{A5S_1} + \frac{ke_{A5S_1}}{2gA_{A5S_1}^{\ 2}} Q_{A5S_1}^2 \;-\; H_{A6S_1} - \frac{ke_{A6S_1}}{2gA_{A6S_1}^{\ 2}} Q_{A6S_1}^2 &= 0 \\
H_{M_4} + \frac{ke_{M_4}}{2gA_{M_4}^{\ 2}} Q_{M_4}^2 \;-\; H_{M_6} - \frac{ke_{M_6}}{2gA_{M_6}^{\ 2}} Q_{M_6}^2 &= 0 \\
H_{M_3} + \frac{ke_{M_3}}{2gA_{M_3}^{\ 2}} Q_{M_3}^2 \;-\; H_{M_5} - \frac{ke_{M_5}}{2gA_{M_5}^{\ 2}} Q_{M_5}^2 &= 0 \\
H_{M10} \;-\; H_{pump} &= 0
\end{aligned}
\qquad (5)
$$

where subscript A_jS_1 refers to the inlet segment of bay j and H_{pump} is the inlet pressure supplied by the pump. Note that the frictional losses are built into Eqs. 2 and 4 used to estimate H_{AjS_1} and H_{M_i}. A root finding algorithm is used to solve Eq. (5) for the inlet pressure of the last lateral of the bays, and hence pressures at the inlet and outlet of the various segments. This implies that, for a given inlet pressure H_{in} to the irrigation network (which is the same as H_{M10} for the hypothetical case), the pressures at various emitter locations within the system can be determined. The individual emitter discharges can then be estimated, and by adding them, the total discharge (Q_{in}) is obtained, and hence the system rating curve (H_{in}-Q_{in}). Superimposing the system rating curve on the pump performance curve, the pump operating point is determined. Should a bay be turned off, its Q value is set to zero and the respective root equation is eliminated from the solution. Turning off bays A1 and A5 for example will eliminate the firstand third equations, and only 4 roots corresponding to the remaining bays will be determined.

Results and Discussion

Emitter Discharge and Emitter Insertion Head Loss Coefficient

Thirteen emitters from different lateral rolls were tested at a CQUniversity laboratory and their rating curves are presented in Fig. 7. Three distinctive rating curves were identified, the emitters grouped according their rating curve. Note that two of the rating curves (Figs. 7a and 7b) refer to the same emitter specification so they were expected to behave similarly but found otherwise. Perhaps, they come from different manufacturing batch. It is observed that, for one set of the 2.1 l/h emitters (Fig. 7a), the average emitter discharge (q) for the recommended pressure head range of 10-35 m is slightly above 2.2 l/h, about 5% higher than the advertised value. Also significant is the high q value for pressures under 10 m, particularly the peaks between 2.3 l/h and 2.5 l/h that occur around 5.5 m head. For the second set of the 2.1 l/h emitters (Fig. 7b), q for the recommended pressure range is about 2.3 l/h, being nearly 10% higher than the advertised value. As seen in Fig. 7c, the 2.4 l/h emitter q value appears to be constant at 2.4 l/h within the recommended pressure range, but rises to a peak of around 2.65 l/h for a pressure head of 5 m. These findings are for a small sample of emitters, so there was a need to investigate the q value using long laterals and bays. What is clear though is that the emitters open at a pressure head as low as 4 m.

Pressure gauges installed on the top dripline of bays F6 and F8 were used to assess the emitter average discharge and the insertion head loss coefficient (α) in Eq. (2). Attention was focused on the expected operating pressures of the laterals. Table 1 presents the results of the emitter characteristics identification experiments using the flowmeter (FM) and the water meter (WM) to measure the flowrates through the laterals. As observed for the single emitter test results, inlet pressure heads under 10 m tended to produce slightly higher flowrates (about 2-5%) compared with the case where

289 all emitter pressure heads are above 10 m. Also, the mean q values between 2.1 l/h and 2.25 l/h are
290 consistent with the single emitter results (Fig. 7a) and a value of 2.2 l/h can be used as a
291 representative value.

292 With the knowledge of the elevation differences and the dripline blank tubing friction factor,
293 the α parameter was obtained by solving Eq. (2) as the only unknown using the observed mean emitter
294 discharge and the inlet and end pressures given in Table 1. While the different sets of data generated
295 significantly varying α values, the average of 0.336 is not far from the published value of 0.36. Fig.
296 8 presents the sensitivity of the α parameter to the inlet pressure for a fixed end pressure, and also
297 the effect of α and q parameters on the pressure distribution along the drip lateral. It is noted that the
298 α parameter is very sensitive to the inlet pressure for a fixed end pressure as demonstrated in Fig. 8a
299 for the first data set in Table 1. For this same data set, the distribution of pressure along the lateral
300 for a fixed emitter discharge (Fig. 8b) indicated that, as α increases, the required inlet pressure to
301 generate the same end pressure also increases. The same is true where α is fixed and q is varied (Fig.
302 8c). The pressure distribution profiles are not significantly different for less than 10% variation in α
303 or in q. In essence, both emitter parameters are strongly negatively correlated and a decrease in one
304 can compensate for an increase in the other to achieve the same pressure distribution profile. This is
305 expected as an increase in either variable causes an increase in head losses in the lateral. The
306 effectiveness of the lateral hydraulic model using only inlet and end pressures was tested using the
307 data in Table 2 of Gyasi-Agyei (2013). These 100 m long pressure compensating laterals have a
308 published ranges of emitter discharge of 1.96-2.24 l/h, diameter of 12.7-13.1 mm, and α value of
309 0.95-1.12. Results not presented here indicated the estimated α values using the measured average q
310 values of the laterals were very close to the published range. For practical applications, measuring
311 the inlet and end pressures is enough for identifying α values for simulation of the dripline network

312 given the elevation differences and dripline blank tubing friction factor.

313 The lateral parameters were used to simulate pressure at all emitters and the average is
314 presented in the last column of Table 1. Variation of q with average pressure is in agreement with
315 what was observed for the single emitter tests shown in Fig. 7a. Average mean pressure of about 5
316 m recorded the highest average emitter discharge of 2.25 l/s. Beyond 10 m pressure head the
317 average q value increased slightly with average pressure.

318 In this section, bay-wise flow measurements were used to infer q as the higher the flow rate
319 the lower the errors of the flowmeter. To improve measurement accuracy, smaller bays were
320 combined with larger ones to estimate their average q value. To this end, total flow of individual
321 bays of F7, F9 and F10 and the combined flows of F9 and F10 were measured using the flowmeter.
322 Checks were made to sure all emitters were discharging during the experiment. The mean emitter
323 discharges were estimated as the ratio of the total flowrates to the number of emitters and are
324 presented in Table 2. Values of bays F9* and F10* (i.e., bays F9 and F10 not measured
325 independently) were estimated from the combined flowrate of F9_10 and the companion flowrate.
326 For example, flowrate of F10 was subtracted from the flowrate of combined F9_10 to obtain F9*
327 flowrate of 114.9 l/min, and the average q of 2.31 l/h. Assuming that the combined bays' measurement
328 is more accurate, then the margin of error could be estimated as less than 5% which is within the
329 accuracy of the flowmeter. From these bay measurements, a representative average emitter discharge
330 of 2.2 to 2.3 l/h is meaningful. In order not to exceed the pressure limits of the poly pipes and the
331 driplines, smaller bays can be combined with a bigger one to estimate their average q values as done
332 for F9* and F10* in Table 2.

333

334

335 ***Pump Performance Curve***

336 The results of the pump performance curve tests carried out at Site F using both the water
337 meter and the flowmeter are presented in Fig. 9 which shows the variation of pump pressure head
338 with the total flowrate. A third order polynomial was fitted to the discharge-pressure pair data to
339 obtain the pump performance curve. It is interesting to observe that both meters' measurements were
340 very close and either could be used for flowrates estimation. However, the measurement using the
341 water meter to measure volumes over time to estimate the flowrate was laborious. The main
342 observation with the pump performance curve tests is the significant difference between the curve
343 supplied by the manufacturer and the results obtained. The difference decreases with flowrate, with
344 11 m pressure head difference at a flowrate of 50 l/min compared to 6 m difference at a flowrate of
345 300 l/min. Using the supplied pump curve could significantly affect the dripline network simulation
346 results. With the pump performance curve established, the mean q value of the respective bays can be
347 estimated by just measuring the pump pressure. When a combination of bays are turned on, the pump
348 pressure reading and the rating curve will give the total flowrate. Dividing the total flowrate by the
349 total number of emitters gives the average q value. Table 2 compares the measured q values with
350 those obtained by using the pump performance curve for bays F7, F8 and F10. An error of less than
351 3.1% was found.

352 Verification of the use of the pump performance curve to estimate q was carried out using
353 bays B3 and B13, chosen arbitrarily but of different lengths and some distance apart. These bays had
354 pressure gauges installed at the inlet and the distal end of the top laterals for the estimation of q
355 values. Bay B3 was turned on with others and pressures at the pump (P1), as well as the relevant
356 gauge locations, were measured. The pump curve established for Site F was used to estimate the
357 average q value. Results presented in Table 3 indicate q ranges between 2.18 l/h and 2.39 l/h with an

358 average value of 2.28 l/h which is close to the average of 2.31 l/h established for the bays at Site F
359 (Table 2). The total flow for the bay combinations using an average q value of 2.28 l/h and the
360 observed pump pressure head are plotted on the pump curve established for Site F (Fig. 10). As the
361 empirical points of Site B lie closely to the fitted curve, it is a clear indication that the Site F pump
362 performance curve is representative of the Site B pump performance curve.
363

364 ***Drip Network Simulation***

365 Since the estimated α mean value of 0.336 was from the two laterals of length 93.3 m and
366 208 m, and its coefficient of variation (CV) of 55.9% was excessive, it was decided to adopt the
367 published manufacturer's value of 0.36. This α parameter value together with the pump performance
368 curve for Site F were used to simulate flows through the dripline network for the given elevation
369 differences. Sensitivity analysis was, however, carried out using the 9 parameter combinations from
370 the set of q={2.2, 2.3 and 2.4 l/h} and α={0.3, 0.36, 4} for the simulations. Assuming a constant q
371 value, the drip network system curve has a constant total discharge value within the emitter discharge
372 pressure head range with a minimum of 4 m. For each q value, the total discharge of the bay
373 combinations in Table 3 was used to infer the pump input pressure head (H_{pump}, Eq. (5)) from the
374 pump performance curve. It was checked to make sure that the simulated minimum pressure head
375 within the dripline network was above the threshold pressure head of 4 m required to open an emitter,
376 and therefore operating within the pressure compensating regime. Simulated pressures at the gauge
377 locations of Site B were extracted and compared with the observed values given in Table 3. Checks
378 were made during the field data gathering to ensure all emitters were discharging. Fig. 11 shows the
379 comparison of the observed and simulated pressures at the gauge location for the 9 combinations of
380 q and α. Also shown on the plots are the computed performance statistics of root-mean-square-error

(RMSE) and mean-absolute-bias-percentage-error (MABPE) defined as:

$$\text{RMSE} = \sqrt{\frac{1}{N_P}\sum_{j=1}^{N_P}\left[P_S(j) - P_O(j)\right]^2} \quad (6)$$

$$\text{MABPE} = 100\frac{1}{N_P}\sum_{j=1}^{N_P}\left|P_S(j) - P_O(j)\right| / P_O(j) \quad (7)$$

where $P_O(j)$ and $P_E(j)$ are, respectively, the observed and estimated pressures at gauge location j, and N_p is the number of gauges. Noting that the smaller the numerical values of the performance statistics the better the performance, with the parameter combination of q=2.3 l/h and α=0.36 yielding RMSE and MABPE values of 1.5 and 7.3%, respectively, outperforming the other parameter combinations. However, it needs to be noted that different bays may have different average q values and the adequacy of the combination of bays needs to be verified in the field. As seen in Table 3, bay B3 has a high *q* value, thus giving an impression that q=2.3 l/h is the best fit. This method of measuring pressures at strategic locations and optimising the lateral parameters through simulation could be an effective way of identifying the parameters.

From the single lateral measurements, the average *q* value was 2.19 l/h (CV of 2.3%) and the average α value was 0.336 (CV of 55.9%). The coefficient of variation of *q* is quite low and reasonable but that of α is excessively high. Using flow measurements in bays, *q* was estimated between 2.18 l/h and 2.44 l/h with an average value of 2.3 l/h. With the high variability of α, it was decided to use the manufacturer's value of 0.36. Since the adopted value of *a* was slightly above the estimated average of 0.336, it was decided to use a slightly lower *q* value of 2.2 l/h. Note that a slightly higher value of α will compensate for a slightly lower value of *q*. The ball valve opening fraction is not expected to change much whether the *q*-α pair of (2.3, 0.336) or (2.2, 0.36) is used. With the emitter parameters of q=2.2 l/h and α=0.36, bay combinations were simulated. A key

402 determinant of rejection of bay combinations is where the minimum pressure head within the dripline
403 network falls below the emitter opening threshold pressure head of 4 m, in which case feasible
404 solutions to the system of equations (Eq. 5) are not achieved. Table 4 presents the results showing
405 the preferred bay combinations and their respective minimum and maximum pressure heads within
406 the drip network. Some bays experienced excessive simulated pressures (e.g. bays B1, B2, B13, B14)
407 which would need to be controlled using the ball valves installed for each bay.

408 Ball valves introduce minor head loss estimated as a product of a coefficient k_{bv} and the
409 velocity head ($V^2/2g$), with k_{bv} decreasing with the opening fraction. Fig. 12 demonstrates the
410 opening fractions of a quarter turn (90^o) ball valve. k_{bv} values for opening fractions of 1/3, 2/3 and 1
411 of 200, 5.5, and 0.05, respectively, obtained at https://www.engineeringtoolbox.com/minor-loss-
412 coefficients-pipes-d_626.html were fitted with an exponential function shown in Fig. 13 and
413 interpolated for the required k_{bv} value for a given opening fraction. Table 4 gives the velocity head
414 at the entry of the individual bays and the ball valve opening fraction to drop the maximum pressure
415 head values to below 25 m. As an example calculation, consider the B1_2_5 bay combination. Bay
416 B1 has a total flowrate of 34.1 l/min and, therefore, the velocity head in the 25 mm sub-main (entry
417 to the bay) is 0.0683 m. Starting at the fully opened position, the ball valve opening fraction is
418 decreased in steps of 1% until the pressure head drops to below 25 m. At a 0.36 opening fraction, k_{bv}
419 is obtained from Fig. 13 as 172.6, and thus causes a pressure head drop of 172.6*0.0683=11.8 m.
420 This leads to a maximum pressure in bay B1 of 35.8-11.8=24 m for a simulated ball valve opening
421 fraction of 0.36.

422 Table 4 presents the opening fractions to drop the dripline network pressure heads to the
423 adjusted maximum pressure values shown in the last column. The bay combinations and operating ball
424 valve opening fractions were determine through simulation, and using q=2.2 l/h which is an uncertain

425 value for an individual bay. Provision was therefore made in case the field officers found that the
426 combination of bays given were not adequate due to the uncertainty of the emitter parameters. When
427 q=2.3 l/h was used, only bay combinations F2_7 and F4_5 did not meet the minimum pressure head
428 requirement of 4 m. However, should this be the case in the field, then the bays would be recombined
429 as (F1_2_9, F 3_6, F 4, F 5, F 7, F 8, F 10_11) which meet the minimum pressure head
430 requirement, with an associated increase in walking distance between bays F1_2 and F9 for the
431 purpose of monitoring the ball valves but with the irrigation times staying the same. For bays F7 and
432 F8, a further 1% reduction in the opening fraction dropped the minimum pressure head to below the
433 threshold value, so the maximum pressure heads were kept above 25 m but within the recommended
434 pressure head range of the emitters. It needs to be stressedthat because geometric controls dictated the
435 bay length, adding an additional bay to a combination of bays shown in Table 4 produced non-
436 feasible solutions of the hydraulic equations.
437
438
439 **Conclusions**
440
441 This paper presents simple methods for validating the emitter characteristics of a new dripline
442 product used on a newly constructed flood levee to aid in the establishment of grasses to control
443 erosion on the batters. It was also necessary to validate the pump performance curve for proper design
444 and simulation of the dripline networks. The dripline networks consisted of several bays which had
445 different lengths and numbers of lateral rows as dictated by fence lines of property boundaries and
446 access road ramps constructed for crossing the levee from one side to the other. Due to pressure
447 limitations on the driplines, and the different sizes of the bays within a drip network which caused

448 significant variations in the pressure distribution, ball valves were necessary to control the bay
449 pressure heads to stay within acceptable limits.

450 Individual emitters were tested for their rating curves in a laboratory. A water meter and an
451 ultrasonic flowmeter were used to assess the pump performance curve as well as the average emitter
452 discharge for lateral lengths and bays. A step-by-step approach in which the hydraulic model is
453 applied to segments, and taking into account all losses, was adopted. Pressure measurements at
454 strategic locations and simulation of flows through driplines networks consisting of combination of
455 bays of different sizes were used to identify the emitter parameters.

456 The findings of the study are the following:

457 • The emitter tests indicated that the average emitter discharge could exceed the supplier's value
458 by as much as 10%, and also the emitter discharge tends to be higher between the opening
459 threshold pressure head of 4 m and 10 m.

460 • The emitter insertion head loss coefficient can be estimated by just measuring the inlet and the
461 distal end pressures of the lateral with the knowledge of the elevation difference and the blank
462 dripline friction factor. While the emitter insertion head loss exhibited considerable variability
463 (0.117 – 0.753), the average value of 0.336 was close to the supplier's value of 0.36.

464 • A more representative way of the assessing the average emitter discharge could be by
465 measuring the total flow through bays, although it needs to be ensured that all emitters are
466 discharging. In order not to exceed pressure head limits, smaller bays could be combined with
467 bigger ones for the estimation of their representative average emitter discharge.

468 • For the pump type used, the supplier's performance curve was overestimated by 11 m pressure
469 head for a flowrate of 50 l/min which decreased to 6 m for a flowrate of 300 l/min, calling for
470 the need to validate manufacturer's pump performance curves.

- With the estimated pump performance curve, the average emitter discharge could easily be estimated by just reading the pressure at the pump outlet when respective bays are opened.
- An effective framework for identifying the emitter parameters through comparison of observed and simulated pressures at strategic locations within the dripline network has been presented. With this method there is no need for flow measurements.
- With effective emitter parameters, simulations were used to predict pressure distribution within the dripline network, and sections violating the pressure head limits were identified. This enabled optimum combination of bays to be operational at the same time.
- Simulation results also revealed excessive bay inlet pressure heads and the corresponding ball valve opening fractions required to drop the inlet pressure to an acceptable limit for each bay were estimated.

Acknowledgements

This research was funded by Maranoa Regional Council (MRC), Queensland, Australia, and this support is gratefully acknowledged. Comments by the reviewers were very helpful and gratefully acknowledged.

References

Bhattarai, S.P., Fox, J, Gyasi-Agyei, Y. (2008). "Enhancing buffel grass seed germination by acid treatment for rapid vegetation establishment on railway batters." *J. Arid Environments*, 72, 255-262.

494 Baiamonte, G. (2016). “Simple Relationships for the Optimal Design of Paired Drip Laterals on
495 Uniform Slopes.” *J. Irrig. Drain. E-ASCE*, 142(2), doi: 10.1061/(ASCE)IR.1943-
496 4774.0000971, 04015054.
497 Baiamonte G. (2018). “Advances in designing drip irrigation laterals.” *Agric. Water Manage.,*
498 199: 157–174, https://doi.org/10.1016/j.agwat.2017.12.015.
499 Carrión F, Tarjuelo J. M., Hernández D., Moreno M. A. (2013). “Design of microirrigation subunit
500 of minimum cost with proper operation.” *Irrig. Sci.* 31, 1199-1211. doi 10.1007/s00271-013-
501 0399-8.
502 Demir, V., Yurdem, H., and Degirmencioglu, A. (2007). “Development of prediction models for
503 friction losses in drip irrigation laterals equipped with integrated in-line and on-line emitters
504 using dimensional analysis.” *Biosyst. Eng.*, 96 (4), 617-631.
505 Fernández García, I., Montesinos, P., Camacho Poyato, E., and Rodríguez Díaz, J.A. (2015).
506 “Energy cost optimization in pressurized irrigation networks.” *Irrig. Sci*, doi: 10.1007/s00271-
507 015-0475-3.
508 Fox, J, Bhattarai, S.P., Gyasi-Agyei, Y. (2011). “Evaluation of different seed mixtures for grass
509 establishment to mitigate soil erosion on steep slopes of railway batters.” *J. Irrig. Drain. Eng.,*
510 137, 624; doi:10.1061/(ASCE)IR.1943-4774.0000319.
511 Gyasi-Agyei, Y., Sibley, J., and Ashwath, N. (2001). “Quantitative evaluation of strategies for
512 erosion control on a railway embankment batter.” *Hydrol. Process.*, 15, 3249- 3268.
513 Gyasi-Agyei, Y. (2003). “Pond water source for irrigation on steep slopes.” *J. Irrig. Drain. Eng*.,
514 129(3), 184-193.
515 Gyasi-Agyei, Y. (2004a). “Optimum use of biodegradable erosion control blankets and waste
516 ballast (rock) mulch to aid grass establishment on steep slopes.” *J. Hydrol. Eng*., 9(2), 150-

159.

Gyasi-Agyei, Y. (2004b). "Cost-effective temporary microirrigation system for grass establishment on environmentally sensitive steep slopes." *J. Irrig. Drain. Eng*., 130(3),218-226.

Gyasi-Agyei, Y. (2007). "Field scale assessment of uncertainties in drip irrigation lateral parameters." *J. Irrig. Drain. Eng*., 133(6), 512-519.

Gyasi-Agyei, Y. (2011). "Compatibility assessment of drip irrigation laterals." *J. Irrig. Drain. Eng*., 137(9), 610-615.

Gyasi-Agyei, Y. (2013). "A Bayesian approach for identifying drip emitter insertion head loss coefficients." *Biosyst. Eng.*, 116 (1), 75-87.

Hathoot, H. M., Al-Amoud, A. I., and Mohammad, F. S. (1993). "Analysis and design of trickle-irrigation laterals." *J. Irrig. Drain. Eng*., 119(5), 756–767.

Hathoot, H. M., Al-Amoud, A. I., and Al-Mesned, A. S. (2000). "Design of trickle irrigation laterals considering emitter losses." *Irrig. Drain*., 49(2), 1–14.

Juana, L., Rodriguez-Sinobas, L., and Losada, A. (2002). "Determining minor head losses in drip irrigation lateral. I: Methodology." *J. Irrig. Drain. Eng*., 128(6), 376–384.

Kang, Y., and Nishiyama, S. (1996). "Analysis and design of microirrigation laterals." *J. Irrig. Drain. Eng*., 122(2), 75–82.

Martí, P., Provenzano, G., Royuela, Á., and Palau-Salvador, G. (2010). "Integrated emitter local loss prediction using artificial neural networks." *J. Irrig. Drain Eng*., 136(1), 11–22.

Provenzano, G., Di Dio, P., and Palau-Salvador, G. (2007). "New computational fluid dynamic procedure to estimate friction and local losses in coextruded drip laterals." *J. Irrig. Drain. Eng*., 133(6), 520-527.

Vallesquino, P., and Luque-Escamilla, P. L. (2002). "Equivalent friction factor method for

hydraulic calculation in irrigation laterals." *J. Irrig. Drain. Eng.,* 128(5), 278–286.

Warrick, A. W., and Yitayew, M. (1988). "Trickle lateral hydraulics. I: Analytical solution." *J. Irrig. Drain. Eng.,* 114(2), 281–288.

Winning H. K., and Coole T. (2013). "Explicit friction factor accuracy and computational efficiency for turbulent flow in pipes". *Flow Turbulence Combust*, 90, 1–27.

Wu, I. P., and Gitlin, H. M. (1975). "Energy gradient line for drip irrigation laterals." *J. Irrig. Drain. Eng.,* 101(4), 323–326.

Yitayew, M., and Warrick, A. W. (1988). "Trickle lateral hydraulics. II: Design and examples." *J. Irrig. Drain. Eng.,* 114(2), 289–300.

Table 1: Estimation of the emitter parameters from the lateral lengths.

lateral	flow equipment	length (m)	P_{inlet} (m)	P_{end} (m)	Q (L/min)	q (L/h)	α	P_{ave} (m)
Bay F6 Top	FM	93.9	7.03	4.92	11.8	2.25	0.337	5.47
Bay F6 Top	FM	93.9	29.9	28.1	11.5	2.21	0.222	28.6
Bay F6 Top	WM	93.3	6.33	4.22	11.6	2.25	0.358	4.76
Bay F6 Top	WM	93.3	15.1	13.0	11.0	2.13	0.448	13.6
Bay F6 Top	WM	93.3	20.7	17.9	11.1	2.14	0.753	18.7
Bay F6 Top	WM	93.3	29.5	27.8	11.2	2.17	0.262	28.2
Bay F6 Top	WM	93.3	37.3	35.2	11.6	2.24	0.364	35.7
Bay F8 Top	WM	208	21.5	6.33	25.4	2.20	0.166	10.3
Bay F8 Top	WM	208	29.5	16.5	24.6	2.13	0.117	19.9
		mean	21.9	17.1	14.4	2.19	0.336	18.4
coefficient of variation, CV, (%)						2.3	55.9	

P_{inlet} – inlet pressure of the lateral; P_{end} - pressure of the lateral; α - emitter insertion head loss coefficient; Q – total flow rate; q – average emitter discharge; P_{ave} – average emitter pressure; FW – flowmeter; WM – water meter

Table 2. Estimation of average emitter discharge from total bay flow measurements at Site F.

bay	observed pump pressure (m)	observed flowrate (l/min)	number of emitters	observed average emitter discharge q (l/h)	pump performance curve estimated q (l/h)	% error in q
F7	52.7	133.4	3483	2.30	2.30	0.1
F9	56.3	121.3	2985	2.44	2.37	-3.0
F10	53.4	133.3	3450	2.32	2.27	-2.2
F9_10	29.5	248.3	6435	2.32	2.24	-3.1
F9*	NA	114.9	2985	2.31	NA	NA
F10*	NA	127.0	3450	2.21	NA	NA

*flowrates were estimated from the F9_10 flowrate and the companion bay

Table 3. Measured gauge pressures and estimation of average emitter discharge from pump pressure measurements at Site B.

bays	N	P1 (m)	P6 (m)	P7 (m)	P8 (m)	P9 (m)	Q (l/min)	q (l/h)	$Q_{2.28}$ (l/min)
B3	3113	54.8	*	*	-	-	124.1	2.39	118.3
B3_13	4589	43.6	35.2	33.1	38.7	37.6	174.7	2.29	174.4
B3_13_14	6065	33.7	22.5	23.9	26.7	26.4	220.2	2.18	230.5
B3_4	7315	23.9	8.44	10.6	-	-	269.2	2.21	278.0
B3_11_13	7852	17.6	5.63	7.03	9.14	8.44	304.6	2.33	298.4

N – number of emitters for the bay combinations; P1 – gauge 1 pressure reading; Q – total flow rate; q – calculated average emitter discharge; $Q_{2.28}$ - total flow rate using q = 2.28 l/h
*pressures exceeded the 42 m limits of the gauges.

Table 4. Ball valve opening fraction required to adjust the maximum drip network pressure to an acceptable limit.

combined bays	estimated pump pressure (m)	bay no.	bay discharge (l/min)	dripline network min. pressure head (m)	dripline network max. pressure head (m)	velocity head at bay inlet (m)	ball valve opening fraction	adjusted drip network max. pressure (m)
Site B								
B1_2_5	37.7	1	34.1	34.3	35.8	0.07	0.36	24.0
B1_2_5	37.7	2	13.6	34.5	36.2	0.01	0.21	24.0
B1_2_5	37.7	5	150.7	21.6	28.9	1.33	0.68	24.6
B3_6	26.5	3	114.1	16.2	19.5	0.77	1.00	19.5
B3_6	26.5	6	137.5	11.9	17.5	1.11	1.00	17.5
B4	47.8	4	154.1	31.3	39.7	1.39	0.58	24.1
B7_8	36.7	7	67.8	27.7	29.7	0.27	0.54	24.7
B7_8	36.7	8	135.9	23.0	28.0	1.08	0.69	24.9
B9_10	31.6	10	135.9	17.2	22.2	1.08	1.00	22.2
B9_10	31.6	9	94.5	20.7	22.2	0.53	1.00	22.2
B11_13	43.8	11	119.6	33.5	36.9	0.84	0.56	24.8
B11_13	43.8	13	54.1	37.6	39.6	0.17	0.41	23.6
B12_14	45.8	12	110.4	36.1	38.8	0.72	0.53	23.9
B12_14	45.8	14	54.1	39.8	41.7	0.17	0.40	23.7
Site F								
F4_5	32.3	4	100.8	9.1	20.4	0.60	1.00	20.4
F4_5	32.3	5	121.0	6.3	20.4	0.86	1.00	20.4
F3_6	28.2	3	125.8	12.4	17.3	0.93	1.00	17.3
F3_6	28.2	6	115.9	12.5	16.3	0.79	1.00	16.3
F2_7	41.5	2	53.5	34.7	36.4	0.17	0.43	24.2
F2_7	41.5	7	127.6	6.9	31.7	0.96	0.79	30.9
F1_8	41.5	1	53.5	34.8	36.5	0.17	0.43	24.3
F1_8	41.5	8	127.6	9.3	31.7	0.96	0.68	28.6
F9_10	30.2	10	126.4	19.5	25.3	0.94	0.85	25.0
F9_10	30.2	9	109.2	22.0	25.8	0.70	0.76	24.9
F11	53.8	11	130.0	41.1	47.4	0.99	0.52	24.0

Fig. 1. Roma township showing location of the airport and levee sites; the yellow short lines delimit the extent of the sites and the black dots are chainages in m.

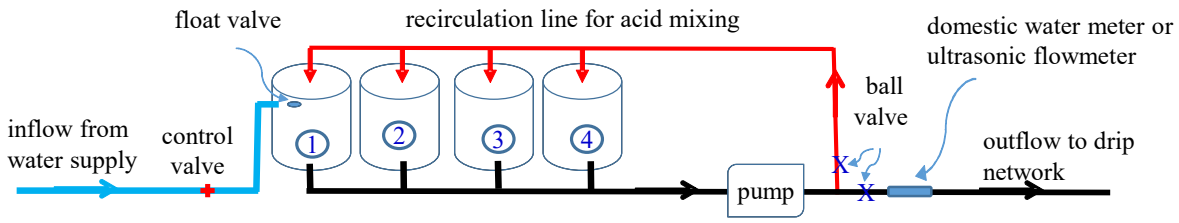

Fig. 2. Water supply and acid mixing set up for 4 tanks in parallel arrangement at Site F.

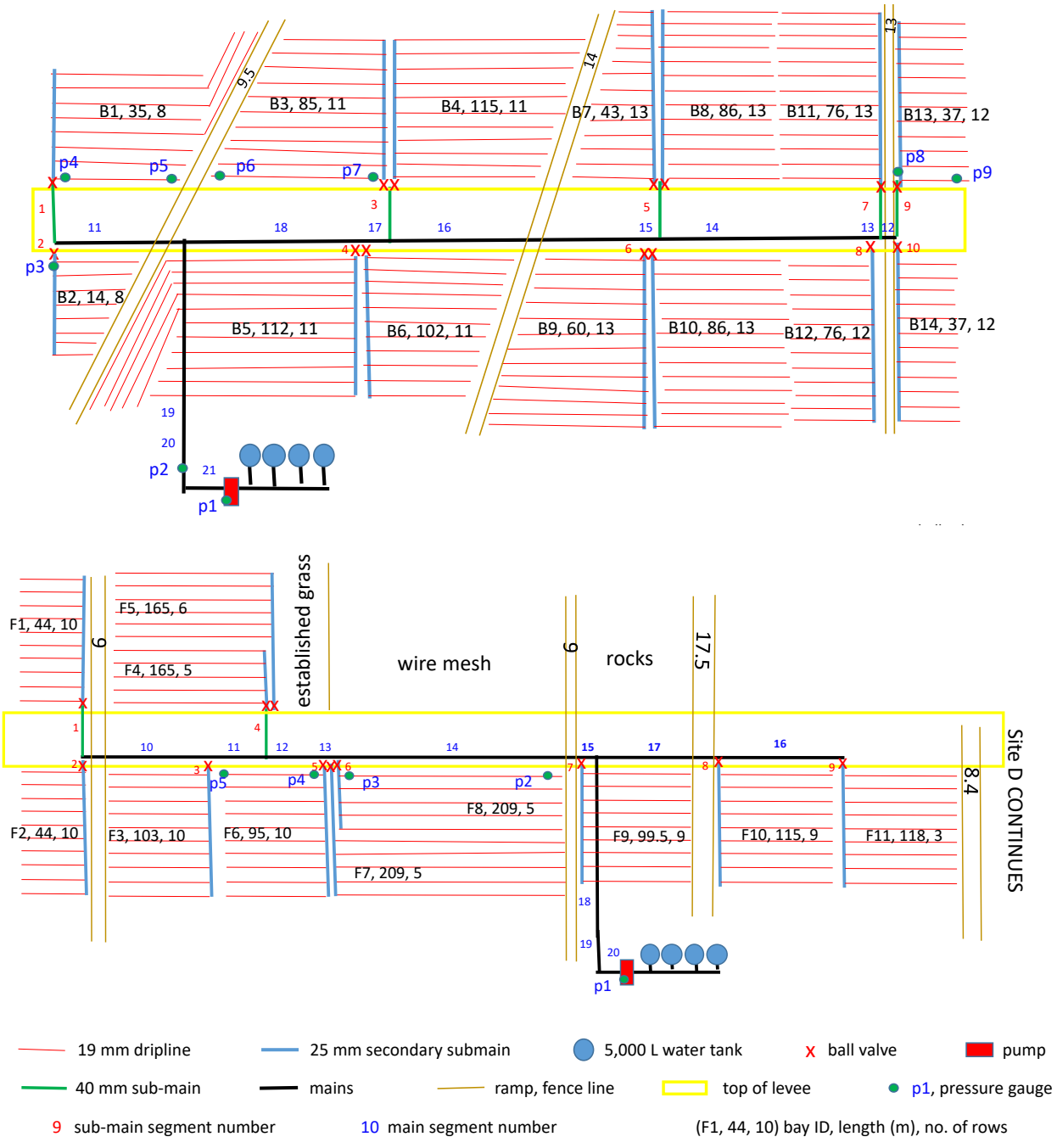

Fig. 3. Dripline network layouts for Sites B and F.

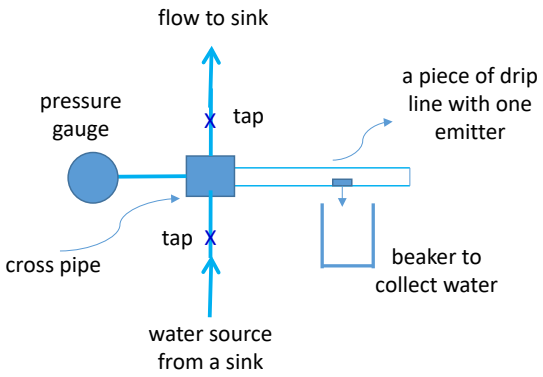

Fig. 4. Set up for establishing the emitter rating curve at a CQUniversity laboratory in Rockhampton, Australia.

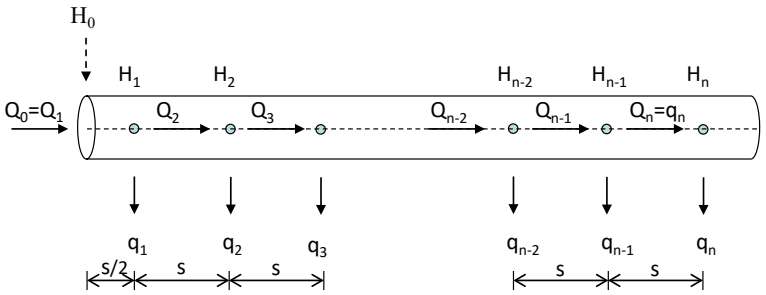

Fig. 5. Hydraulic features of a single lateral.

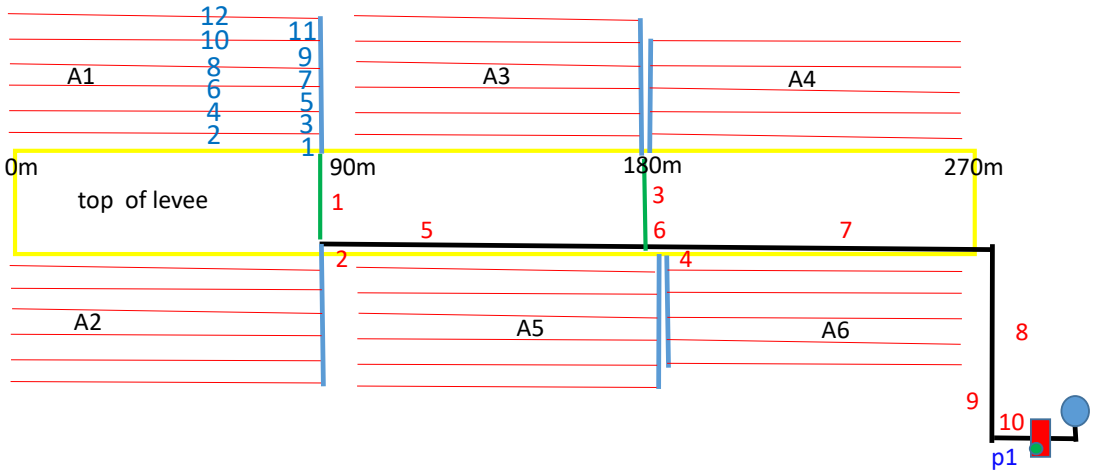

Fig. 6. A hypothetical Site A irrigation network having 6 bays numbered from A1 through A6; segments for bay A1 are numbered in blue, and segments numbered in red are the submain and main for the whole network.

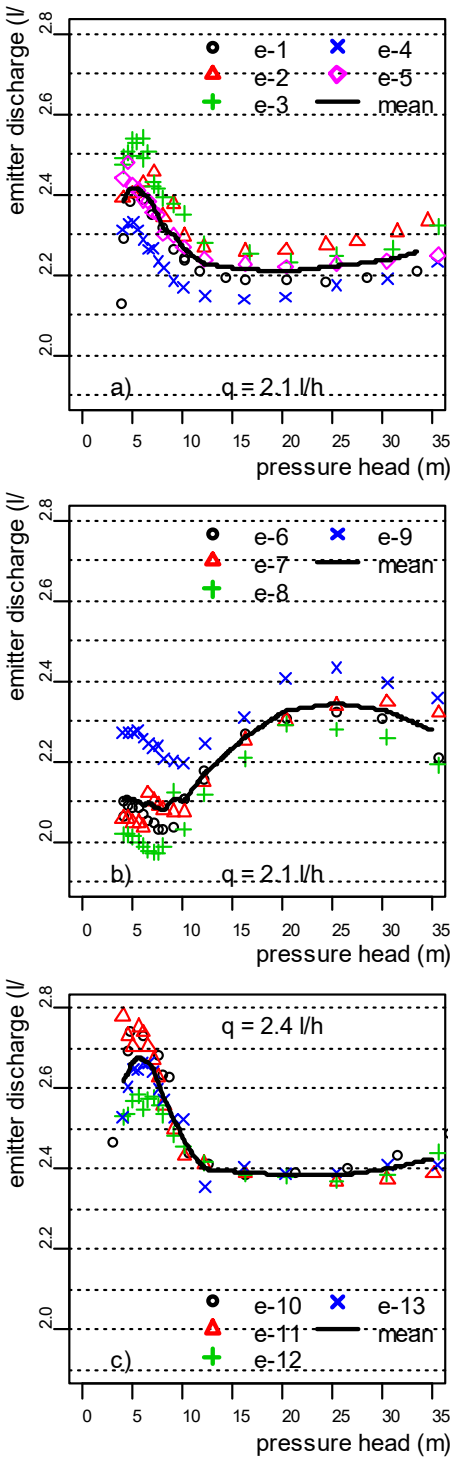

Fig. 7. Emitter rating curves; a) and b) are for the 2.1 l/h and c) is for the 2.4 l/h specification driplines.

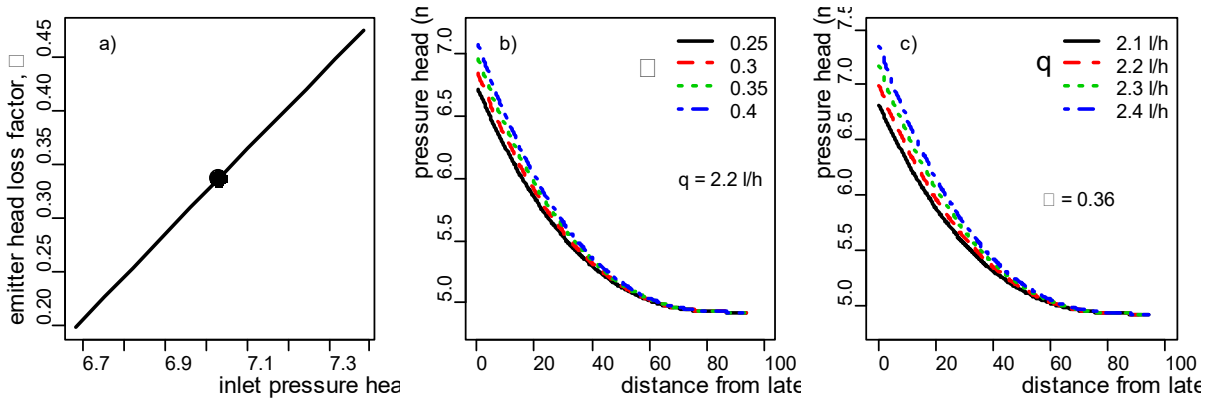

Fig. 8. Characteristics relationships: a) sensitivity of the emitter insertion head loss parameter (α) to inlet pressure for a fixed end pressure; b) the effect of α on pressure distribution along the drip lateral; and c) the effect of emitter discharge (q) on pressure distribution along the drip lateral.

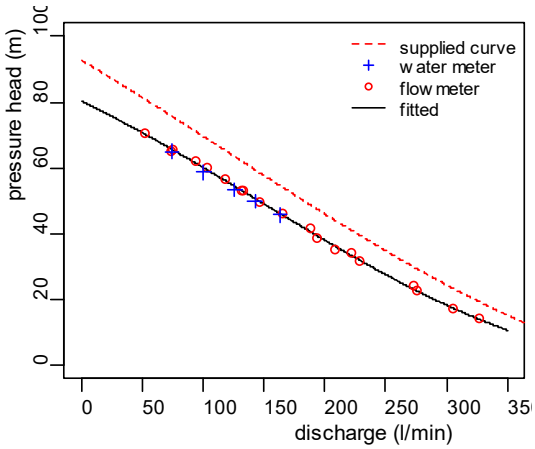

Fig. 9. Pump performance curve tests carried out at Site F using both the water meter and the flowmeter.

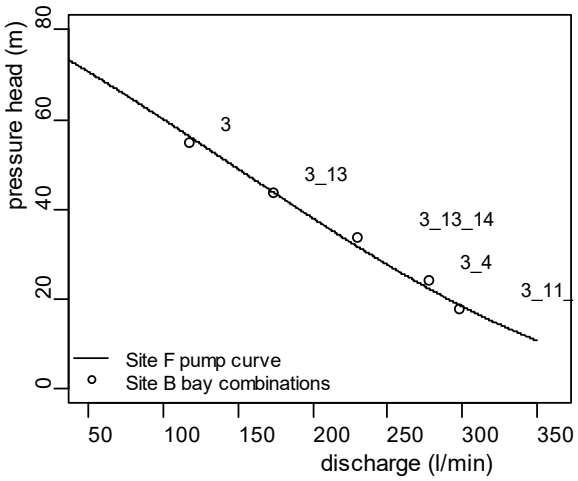

Fig. 10. Pump pressure measured at Site B for bay combinations (indicated against the circled points) using an average emitter discharge of 2.28 l/h and superimposed on the pump rating curve at Site F.

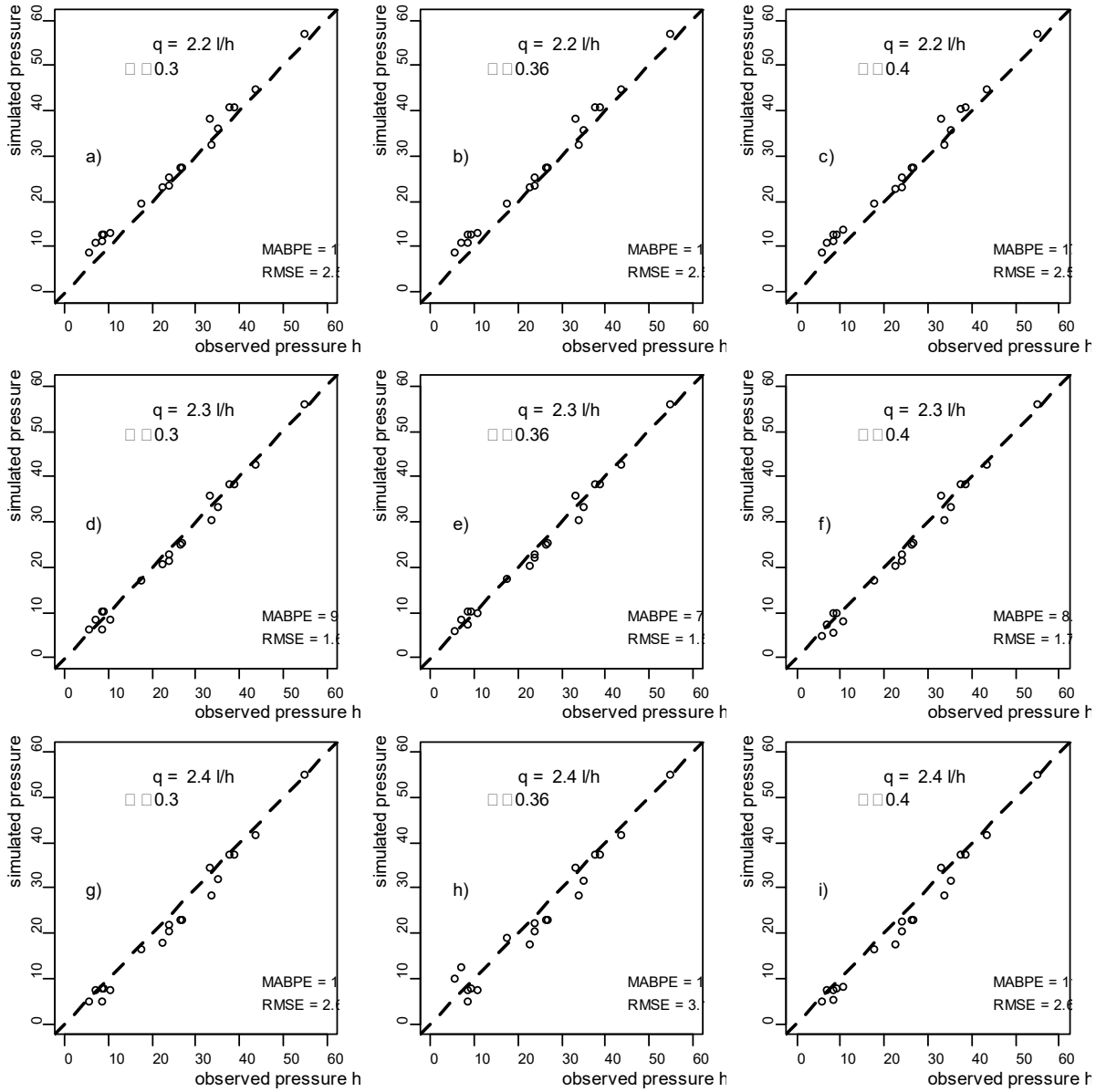

Fig. 11. Comparison of observed and simulated pressure heads at locations within the irrigation network of Site B; line of perfect match shown as dashed lines.

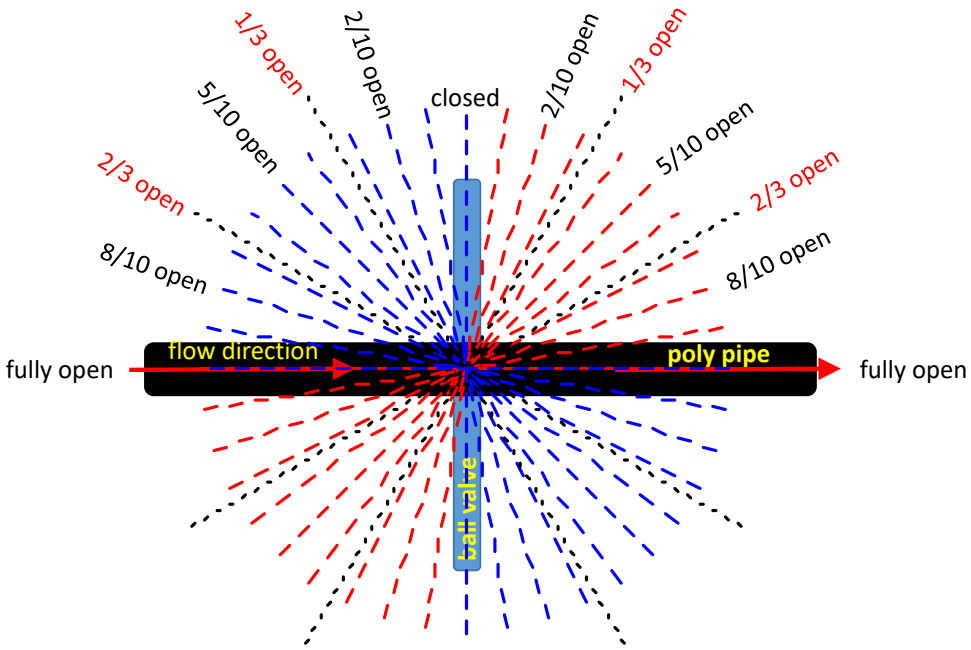

Fig. 12. Ball valve opening fraction positions.

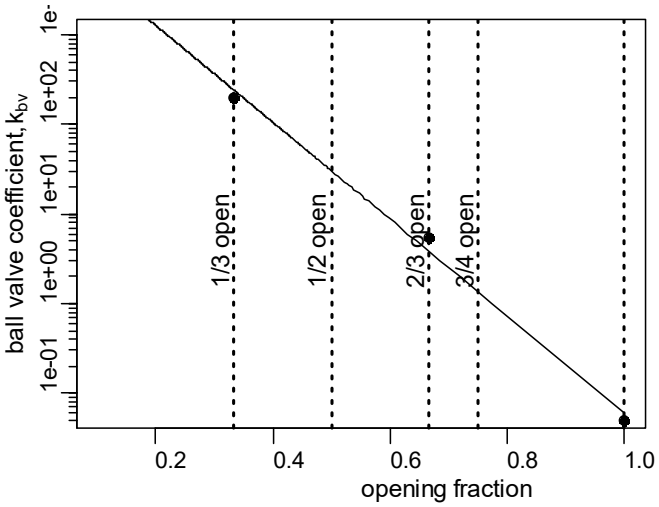

Fig. 13. Ball valve coefficient against opening fraction curve.